

A Medium Resolution Near-Infrared Spectral Atlas of O and Early B Stars

M.M. Hanson^{1,5}, R.-P. Kudritzki², M.A. Kenworthy^{1,3}

J. Puls⁴, A.T. Tokunaga²

ABSTRACT

We present intermediate resolution ($R \sim 8,000 - 12,000$) high signal-to-noise H - and K -band spectroscopy of a sample of 37 optically visible stars, ranging in spectral type from O3 to B3 and representing most luminosity classes. Spectra of this quality can be used to constrain the temperature, luminosity and general wind properties of OB stars, when used in conjunction with sophisticated atmospheric model codes. Most important is the need for moderately high resolutions ($R \geq 5000$) and very high signal-to-noise ($S/N \geq 150$) spectra for a meaningful profile analysis. When using near-infrared spectra for a classification system, moderately high signal-to-noise ($S/N \sim 100$) is still required, though the resolution can be relaxed to just a thousand or two. In the appendix we provide a set of very high quality near-infrared spectra of Brackett lines in six early-A dwarfs. These can be used to aid in the modeling and removal of such lines when early-A dwarfs are used for telluric spectroscopic standards.

Subject headings: stars: early type — infrared: stars — stars: fundamental parameters — atlases — techniques: spectroscopic

1. INTRODUCTION

Kleinmann & Hall (1986) were the first to present reasonably-high resolution, high signal-to-noise (S/N) near-infrared (NIR) spectra for cool stars. The first NIR spectral atlas of hot stars was given by Lançon & Rocca-Volmerage (1992). Designed for use in stellar population synthesis models, the Lançon & Rocca-Volmerage atlas lacked adequate resolution for applications in many stellar and galactic programs. A few years later, Dallier et al. (1996) and Hanson et al. (1996) presented H -band and K -band spectral atlases, respectively, which included OB stars with significantly higher resolution and S/N . Numerous NIR atlases of OB stars have been published since that time (Wallace & Hinkle 1997, Lenorzer et al. 2002, for a recent review of all NIR spectral atlases, see Ivanov et al. 2004). The utility of a NIR spectral classification scheme, for hot stars in particular, has proved exceedingly useful for a variety of applications, including studies of very young star forming regions (Bik et al. 2003) and the galactic center region (Najarro et al. 1997, Ghez et

¹Department of Physics, The University of Cincinnati, Cincinnati, OH 45221-0011

²Institute for Astronomy, University of Hawaii, 2680 Woodlawn Drive, Honolulu, HI 96822

³Present Address: Steward Observatory, University of Arizona, 933 Cherry Avenue, Tucson AZ 85721-0065

⁴Universitäts-Sternwarte München, Scheinerstr. 1, D-81679 München, Germany

⁵Visiting astronomer, The Subaru Observatory and The Very Large Telescope

al. 2003; Najarro et al. 2004) as well as distant massive clusters through out the Galaxy (Hanson, Conti & Howarth 1997, Blum, Daminieli & Conti 1999; Figer et al. 2005). Furthermore, researchers studying heavily reddened high-mass X-ray binary systems (Clark et al. 2003; Morel & Grosdidier 2005) and microquasars (Mirabel et al. 1997, Martí et al. 2000) have found NIR spectral classification to be uniquely valuable.

In light of these successes, our group wishes to push NIR spectral studies of OB stars to a new, more sophisticated level. Our goal is to obtain new, higher resolution and S/N NIR OB spectra to test and guide existing quantitative atmospheric models for OB stars in the NIR regime (Najarro et al. 1998; Kudritzki & Puls 2000 and references therein). In turn, once the atmospheric models have been calibrated to properly predict stellar characteristics based on the NIR spectra of known, UV- and optically-studied stars, it is our hope that they may be used to provide accurate constraints to the characteristics of stars observable only in the NIR. This NIR atlas of well known, optically visible OB stars makes up the sample of high-quality spectra which are being used by our group for a successful NIR qualitative analysis (Repolust et al. submitted).

2. OBSERVATIONS

A list of the stars used for the survey, their position, and salient details of the observations is given in Table 1. When our observations were carried out, reasonably-high-resolution ($R > 8000$) spectrometers which allowed for sufficient spectral coverage were only available on 8- and 10-meter class telescopes. Our targets are exceedingly bright for such a large aperture system. However, these observations are absolutely necessary for the sake of developing and testing quantitative model atmospheres. Furthermore, we needed to start with optically visible, well known O and early-B stars. The OB sample was selected to give reasonable coverage of the temperature and luminosity range of O and early-B stars. The temperature and luminosity range sampled is illustrated in the spectral type versus luminosity class presentation given in Table 2.

There presently are no classification standards in the NIR. Until sufficient numbers of OB stars have been observed in the NIR, it will be too soon to claim any star as a classification standard. The stars selected in this survey are **not** being promoted as standard stars for spectral classification. The targets for this program were selected based on entirely different criteria. The OB supergiant stars observed with the VLT were obtained as part of a study of OB supergiants near the galactic center (Fickenscher, Hanson & Puls, 2004). For ease of the observing run, this required them to be in the vicinity of the galactic center fields being observed. Most of the stars observed with Subaru were hand selected by one of us (J.P.). The Subaru sample was selected to cover a reasonable sampling of effective temperature and gravity, and most importantly, with the expressed desire to model their spectral profiles using modifications to the atmospheric code FASTWIND (Puls et al. 2005). Most of the stars selected have already undergone significant previous spectroscopic modeling in the optical and UV, and did not show any serious irregularities in those analyzes. The very high resolution of these observations are well beyond those typically used for classification in the optical ($R \sim$ few thousand). Spectra for the purpose of classification, no matter the wavelength, are best obtained at more moderate resolutions (see further discussion of this point in §5.2).

2.1. The VLT-ISAAC Spectra

The first of our data came from the Infrared Spectrometer and Array Camera (ISAAC). The instrument is mounted at Nasmyth focus on the 8.2m Unit 1 telescope of the European Southern Observatory’s (ESO) Very Large Telescope (VLT), located on Cerro Paranal in Atacama, Chile (Moorwood 1997). ISAAC employs

a Rockwell Hawaii 1024² array and a single grating. The resolution is set by the slit width. In May and April of 2001, long slit (120”) *H*– and *K*–band spectra were obtained for a number of optically visible late-O and early-B supergiants. All data for this program were obtained in the queue observing mode, spread out over about two months and using approximately 12 hours of VLT queue time. Typically 8 slit positions were obtained, with total on-source integration times of one to a few minutes. A slit-width of 0.3” was used, giving a spectral resolving power of $R \sim 10,000$ in the *H*–band and $R \sim 8,000$ in the *K*–band. Three grating settings, 1.710, 2.085, and 2.166 μm , were used with ISAAC.

2.2. The Subaru-IRCS Spectra

Later that year, we obtained additional spectra at the 8.2-m Subaru Telescope, operated by the National Astronomical Observatory of Japan (Tokunaga et al. 1998) and located at the top of Mauna Kea in Hawaii. We employed the Infrared Camera and Spectrograph (IRCS) installed at Cassegrain focus. IRCS uses two 1024² ALADDIN arrays and offers a cross-dispersed echelle mode for high resolution work. With the present arrays, the cross-dispersed mode does not allow for full spectral coverage, leaving unobserved spectral regions between the echelle orders. For full coverage, two settings can be completed. However, nearly all the important lines for our survey (except the $\lambda 2.0581\mu\text{m}$ HeI line) were observed with a single grating setting.

To achieve the highest resolution, we used the most narrow slit setting (0.15”). This provided a resolution of about 0.5 $\text{\AA}/\text{pixel}$ in *K*, and about 0.4 $\text{\AA}/\text{pixel}$ in *H*. In practice, we achieved an approximate FWHM of 3.5 pixels, measured through the OH sky emission features, resulting in a final spectral resolution of approximately $R \sim 12,000$. These spectra were obtained over two separate runs, first in November 2001, then later in July 2002, based on the targets’ right ascension. Two nights were granted for each run. The first night was used to obtain just the *K*–band spectra, the second night was reserved for the *H*–band spectra for the same stars. The weather in November 2001 was rather poor; clouds on the mountain had closed just about every other optical observatory. Because our sources are so bright (with *K* magnitudes as large as 2), we managed to get sufficient counts despite the weather. Telluric corrections did prove to be more problematic, however, because of the poor sky conditions. Conditions in July 2002 were also less than ideal, but again, given the brightness of our targets and the 8-m aperture we obtained sufficient counts. Intermittent heavy clouds did lead to some poor telluric corrections in the final spectra for some sources. We failed to get a follow up *H*– band spectrum of HD 15558 during the second night. Also, the *H*–band spectrum of τ Sco, HD 149757, was somehow corrupted. Regrettably, a trustworthy spectrum proved irretrievable from our raw data.

3. REDUCTION OF THE SPECTRA

All VLT-ISAAC spectra were reduced using IRAF¹ routines. Subsequent analysis of the Subaru spectra was done using routines written in PerlDL².

The OB stars and a few telluric standards (more on that presently) were observed with the traditional long-slit AB “nodding” pattern on both telescopes (with a small, few arcsecond jitter to better sample the

¹IRAF is distributed by the National Optical Astronomy Observatories, which are operated by the Association of Universities for Research in Astronomy, Inc., under cooperative agreement with the National Science Foundation.

²homepage at <http://pdl.perl.org/>

detector). This allows quick and effective subtraction of background emission when the A slit position is subtracted from the B slit position several arcseconds away (and vice versa). For all stars observed with the VLT, four AB pairs were obtained, giving us 8 individual spectra. For the November 2001 Subaru run, three ABBA sets were used. This was reduced to just 2 ABBA sets for the July 2002 run. Each two-dimensional spectral image was bias (and other instrumental effects) subtracted before flat fielding. For all spectra, regardless of telescope, dark frames and flat field frames were averaged together to form a master dark and flat frame. Then AB pairs are subtracted to remove the last of the sky emission. Finally, each individual spectrum from the set were extracted, weighted and scaled before being averaged, using a 3-sigma rejection. Telluric OH emission lines (Rousselot et al. 2000), ubiquitous throughout the spectral range of our data, were used for wavelength calibrations.

The Earth’s atmosphere introduces a myriad of absorption lines into ground-based, NIR spectra, and these need to be removed (Fig. 1). Because the features are complex and continuously changing, *in situ* measures, via a telluric standard star, are the best means of constraining their character. Owing to their near featureless continuum (with the very big exception of the Brackett series of Hydrogen), late-B and early-A dwarf stars are frequently used in this regard. For each target star observed with the VLT-ISAAC, a telluric standard star was observed either just before or after the target object. This telluric star was selected to exhibit the same airmass (to within a few hundredths usually) as the target object, and to lie in the same general sky direction of the target object. AB nodding along the slit was used to observe the telluric stars. Identical procedures were used for the reduction of the telluric stars as was used for the OB stars as outlined above. For the VLT run, we observed a late-B dwarf, matched to each OB target star and put into individual observing blocks (as required for VLT queue observing). We also obtained spectra of a few early-G dwarfs in some of the observing blocks. These early-G dwarfs are used with the NIR spectrum of the Sun to help constrain the Brackett features in the B-dwarf star. Once the Brackett features have been modeled in the late-B dwarf, they can be divided from the late-B dwarf spectrum to create the telluric spectrum. The telluric spectrum is then finally divided from the raw OB target star spectrum (see the Appendix in Hanson et al. 1996).

For the Subaru run, observations were taken in standard visitor mode. A number of early-A dwarfs were observed through out the night on the assumption that they would be used in the removal of telluric features. In the end, however, they had very limited use. For OB stellar lines far from the influence of any Brackett series transitions (HeII, most of the HeI lines, etc.) the A stars were useful to derive the telluric spectrum, but the Subaru spectra had unprecedented S/N and even higher resolution than the VLT-ISAAC spectra. Consequently, any estimated fit for the Hydrogen Brackett lines in the A dwarf stars could not be adequately constrained to derive the OB star hydrogen lines. Ironically, the most ideal telluric standards would be very hot stars, because they have the fewest, weakest lines of all normal stars. In the end, we were faced with using the OB stars themselves, taken throughout the night, as telluric standards for each other in deriving the Hydrogen Brackett lines. In the infrared, every spectrum is like an equation with two unknowns: the telluric spectrum and the stellar spectrum. Taking additional spectra of other stars does not solve this, even if the telluric spectrum is the same, since every new spectrum is a new equation, but adds an additional unknown (the underlying spectrum of the new star). This is the case ONLY in the Brackett region because every star shows a unique Brackett feature. At some point, one is forced to make an *assumption* about the Brackett line profile in one of the stars (it is our experience that this is preferred over trying to make an assumption about the strength and shape of the numerous telluric features that span the Brackett spectral range). This reduces the number of unknowns to equal the number of spectra (‘equations’) and allows for a solution. Typically, a Voigt profile was used as a first, reasonable guess for the most well behaved stars observed during the night: late-O or early-B dwarfs. This ‘solution’ was then propagated through all the

stars observed that night, dividing one against another until one finally resolves the underlying spectrum for all the stars from the night. If problems or inconsistencies are revealed, then a new assumption can be made and propagated through the stars for that night.

3.1. The need for synthesized spectra

Is there any way to know if our assumptions made to model our most ‘normal’ stars are reasonable? What is our likely error? This would be very difficult to determine if we had no idea of the expected profile shapes for our OB stars. Luckily, in conjunction (and as a parallel goal) with the development of this high S/N atlas, our group is also expanding existing sophisticated models of OB stellar atmospheres to predict and produce line profiles in the NIR (Repolust et al. 2005). Once a best guess was made and the underlying spectrum of all the stars was completed, these were compared with synthesized spectra our group created. If our assumptions about the Brackett profile are wrong, then very obvious patterns of inconsistencies would appear in the comparison of data and models. Indeed, it was found that the Br10 line of Hydrogen appeared to be consistently too weak (as compared to the model predictions) for all stars observed in November 2001. We returned to the data, used a stronger line for the primary assumption, and then this solution was propagated through out the night. We found that a more satisfactory fit was obtained for all the star in this particular line after having done this.

But still, what is the expected error in our profiles? Given the brightness of our target (and telluric) stars, flux is not so much a limit to our confidence (indeed we have very high S/N) it is the accuracy of the telluric corrections and the assumptions made in fitting the Brackett features. For the November 2001 ‘inconsistency’, the strength of the Br10 line was increased by approximately 1.5% compared to the continuum. This made a significant difference in the Br10 line as seen in the O4 supergiant, HD 14947 (it was the weakness of the Br10 line in HD 14947 which exposed the problem). But such a small difference was essentially undetectable in the Br10 spectrum of the B2 dwarf, HD 36166. Given the goodness of the fits to the synthesized spectra and the reproducibility of the features using the telluric A-star standards, we expect the HeI and HeII lines to be good to at least 0.5% of the continuum. The Brackett lines pose special problems, as we’ve outlined. We estimate those lines to be good to between 0.5% and 1% through out the wings, and perhaps only good to 1% to even as bad as 2% of the continuum in the line core.

Telluric corrections in the short-K band provide additional challenges. While there is no strong hydrogen line residing here, making early-A dwarfs near perfect telluric tracers between 2 and 2.15 μm , the Earth’s atmosphere becomes increasing problematic below 2.08 μm . Here, very strong and quickly changing telluric absorption is found, predominately due to the ro-vibrational transitions of CO₂. Just the *start* of this very strong absorption is illustrated in Figure 1. The absorption continues to get deeper at shorter wavelengths not given in Figure 1. For a thorough discussion of the special problems posed in this spectral region, see Kenworthy & Hanson (2004). The S/N measures listed in Table 1 represent the average through out most of the spectral range covered for the spectrum, and does not consider that over the CO₂ region, the S/N can drop by 30% or more. Similar telluric noise can also be seen in the *H*–band region, where telluric features become increasingly strong and problematic longward of 1.72 μm (Fig. 1).

4. THE SPECTRA

This atlas contains H - and K -band spectra for 37 OB stars, ranging from O3 to B3, and sampling most luminosity classes over that spectral range. The spectra have been displayed in two ways. All spectra in the atlas are presented in Figures 2 through 8. Here the spectra have been arranged based on temperature so the reader can see the temperature-dependent variations. In Figures 9 through 12, we have presented the spectra grouped by similar temperature, but arranged along varying luminosity. Here the reader can see the luminosity-dependent variations for four differing temperature regimes.

4.1. Line Identifications

The NIR is home to the Brackett Hydrogen series, beginning with Brackett α at $4.052 \mu\text{m}$ (all wavelengths listed are given for air). Over the spectral range covered in this atlas, we see $2.1661 \mu\text{m}$ (4-7) Brackett γ (Br γ), $1.736 \mu\text{m}$ (4-10) Br10, $1.681 \mu\text{m}$ (4-11) Br11 and $1.641 \mu\text{m}$ (4-12) Br12.

Lines of HeI and HeII both exist in the H - and the K -band regions. Within the H -band, one finds absorption due to HeII $\lambda 1.693$ (7-12) and HeI $\lambda 1.700$ ($3p \ ^3P^o - 4d \ ^3D$, triplet). Within the K -band, there exists the lines, HeII $\lambda 2.188$ (7-10), HeI $\lambda 2.1127$ ($3p \ ^3P^o - 4s \ ^3S$, triplet) and $\lambda 2.1138$ ($3p \ ^1P^o - 4s \ ^1S$, singlet). Though our spectral coverage from Subaru does not include this line, still another important He line is the singlet HeI transition, $\lambda 2.0581$ ($2s \ ^1S - 2p \ ^1P^o$). This line is seen in several of our late-O, early-B supergiants observed with ISAAC. The higher resolution and S/N obtained in this atlas allows additional HeI lines to be identified. In late-O and early-B supergiants (Fig. 5, 7, 8, 11 & 12) we see HeI $\lambda 2.161$ ($4d \ ^3D - 7f \ ^3F$, triplet) and at $\lambda 2.162$ ($4d \ ^1D - 7f \ ^1F$, singlet) begins to appear in the blue wing of Br γ .

After Helium and Hydrogen, most OB stars show relatively few spectral features in their NIR spectra. Among the hottest stars, the triplet due to CIV ($3d^2D - 3p^2P^o$) at 2.069, 2.078 and 2.083 is seen. In our O3 supergiant, Cyg OB2 #7, the leading line in this set, at $2.078 \mu\text{m}$, is seen in absorption! A second important metal line seen in the NIR spectra of hot stars is the broad emission feature found at $2.1155 \mu\text{m}$, tentatively identified by Hanson et al. (1996) as NIII (7-8), though may instead (or also) be due to the very similar transition of CIII (7-8). The difficulty in firmly identifying this features comes from the fact that the atoms share a similar structure and the transition identified here originates between very high lying levels. It is expected, based on arguments of relative abundances between N and C, that the feature seen is dominated by NIII, particularly in more evolved stars. Stars where CIII may dominate the profile, would include hotter, less evolved stars which also exhibit strong CIV emission. One can find additional discussion of the $2.1155 \mu\text{m}$ feature in Repolust et al. (2005).

Additional lines previously cataloged in hot stars and seen in our spectra include: $\lambda 2.100 \mu\text{m}$ NV seen in HD 64568, an O3 V((f)), $\lambda 2.137/2.143 \mu\text{m}$ MgII in early-B supergiants, and numerous HeI lines at $\lambda 2.150 \mu\text{m}$, $\lambda 2.161/2 \mu\text{m}$, and $\lambda 2.184 \mu\text{m}$, all seen in late-O and early-B supergiants (see Fig. 8). Because of the high resolution and S/N of our spectra, a few new, unidentified lines have been found. These include absorption lines seen in mid and late-O stars at $\lambda 1.649, 1.651 \mu\text{m}$, an emission feature seen in the O5 If+ star HD 14947 at $\lambda 2.1035 \mu\text{m}$, and several emission features seen clustered around the Br10 line of the O3 If* star, Cyg OB2 # 7. The strongest of these, centered around $\lambda 1.735 \mu\text{m}$, might also be seen in the O4 I(n)f star HD 66811.

4.2. Classification Criteria for Temperature and Luminosity

As with the optical (Walborn & Fitzpatrick 1990), the principal temperature classification criteria for O stars in the NIR is found within the behaviors of the HeI and HeII lines. The strength of the He lines as a function of temperature has been well established based on earlier, lower-resolution work (Hanson et al. 1996; Blum et al. 1997; Hanson et al. 1998), which have quantified its behavior. Ionized Helium, the strongest of the NIR transitions being the HeII (7-10) line at $\lambda 2.1885$, is present in absorption in essentially all O stars, regardless of luminosity class (though it is so weak in O9 V stars it would go undetected in lower quality spectra). By mid-O, neutral Helium emerges (see Fig. 2, 4) and is retained until early-B for dwarf stars (see Fig. 3), but as late as B7 or B8 in supergiants (see Hanson et al. 1996). When both HeII and HeI are present, temperature estimates are at their best.

The unique HeI line at $\lambda 2.0581\mu\text{m}$ is highly sensitive to temperature *and* wind properties. It first appears in absorption in mid- to late-O stars (see Fig. 5, 7), and is frequently seen in strong emission in early-B supergiants (see Fig. 8). Unfortunately, this particular study is unable to shed significant light on its behavior due to the small number of stars observed here. It should be noted that this line lies within a region of the Earth’s atmosphere where interfering telluric absorption is large, and accurate, high S/N profiles are challenging to obtain from the ground.

Unlike the Helium transitions which are unique to hot stars, hydrogen lines are instead ubiquitous to all stars of cosmic abundance. Despite being common, the hydrogen lines serve an important role in constraining characteristics of OB stars. Over the temperature range of this study, the cores of the Brackett transitions, particularly Br10 and Br11, are excellent indicators of gravity. Among stars of similar rotational velocity, stars with lower gravity (higher luminosity), are seen to have much deeper cores. This leads to a *stronger*, larger equivalent width in the Brackett lines in high luminosity O and early-B stars (see Figs. 9, 10, 11 and 12). While some of the HeI lines appear to follow a similar route, their profiles becoming deeper and sharper as luminosity increases in OB stars, much of this profile change is due to a change in rotational velocity (see for example, Fig. 11). This behavior of deepening of the cores in the upper level Hydrogen lines, is entirely explained theoretically. Repolust et al. (2005) explain that the core is simply responding to the Stark-profiles which are a strong function of electron density. Such an effect is only seen in the cores of hydrogen lines with large upper principal quantum numbers. For Br γ , with upper quantum number $n=7$, the effect is less sensitive and it is entirely insensitive in H α where the cores are instead dominated by Doppler-broadening. Thus the profile shape of the cores in Br10 and Br 11 provide a sensitive indicator of gravity (luminosity), provided broadening from rotation is already constrained ³. In high gravity OB stars, there is greater absorption in the wings of the higher order Brackett profiles (see in particular Fig. 12). It is important to recognize that without adequate resolution these subtle changes in Brackett γ and Helium line profiles which trace luminosity would be lost.

The metal lines of CIV and NIII can be used as vague temperature indicators and are particularly useful with low S/N spectra or in spectra plagued with very strong nebular emission lines rendering the helium lines unusable. CIV appears in emission starting around O4-O5, and is seen down to about O7 in dwarf stars (though it is weak and may be missed with low quality spectra). This atlas lacks adequate sampling of the O8 spectral sequence in luminosity. However, the existence of CIV in O8 supergiants, and its increasing strength with increasing luminosity, was shown in Hanson et al. (1996). NIII is seen in all early-O stars,

³Unfortunately, a higher luminosity implies a larger mass-loss rate, so that the profiles might become refilled by wind-emission and thus weaker again. One such example is given in Fig. 9, if one compares Br12/11/10 from Cyg OB 8c (O5 If) with those from HD 14947 (O5 If+).

down to about O7 in the dwarfs, and possibly as late as O8 in supergiants, though it is heavily blended with the HeI $\lambda 2.112/3$ line. In very luminous late-O stars, the triplet $\lambda 2.1127$ ($3p\ ^3P^o - 4s\ ^3S$) remains in absorption, while the singlet $\lambda 2.1138$ ($3p\ ^1P^o - 4s\ ^1S$) line goes into emission (Najarro et al. 1994). As previously discussed, a confident identification of the line at $2.1155\ \mu\text{m}$ (whether it be CIII or NIII) is still lacking. For purposes of spectral classification, this is not an issue. For purposes of spectral analysis, it will be.

5. DISCUSSION

In the mid-90s, several papers presented low and moderate resolution NIR spectra of stars. Previous to spectroscopic studies, the only tool for determining the characteristics of heavily reddened stars was through broadband NIR colors. While such measures are effective for constraining cool stars, NIR photometric colors becoming increasingly degenerate for hot stars. It was pointed out by Massey et al. (1995) that UBV colors were degenerate for O stars, necessitating the need for MK classification for proper determinations of mass functions within OB clusters. For JHK colors, the degeneracy begins at A stars. The development of even a low resolution classification system for the NIR has proved enormously useful for those studying hot stars behind significant interstellar extinction.

However, with near-infrared spectrometers becoming more sophisticated, it was time to push the observations *and theory* to a complementary level. Our groups theoretical work shows that with increased resolution and S/N rather accurate physical characteristics of hot stars can be derived with NIR spectra alone (Repolust et al. 2005). But this does require an analysis be used in conjunction with theoretically derived line profiles to achieve such accurate characteristics.

5.1. What level of S/N and resolution will be required for a quantitative analysis?

It's unlikely that typical researchers will have the luxury that this study possessed: using an 8-m class telescope to observe exceedingly bright, single sources, void of nebular contamination. In many astrophysical situations, nebular emission can contaminate important diagnostic lines (most usually $\text{Br}\gamma$ and $\lambda 2.058\ \mu\text{m}$ HeI), rendering them useless. In the most extreme situations, where the extinction to the massive star is exasperated by thermal emission in the NIR from nebular or circumstellar material, all absorption lines may be undetectable. It is clear that both NIR spectral analysis and classification will have very real and frustrating limits in their application to massive young stellar objects (Hanson et al. 1997; Blum et al. 2001; Bik et al. 2005a). In incidences where there is significant contamination from thermal emission, this has an effect much like reducing the S/N. Imagine if one obtained a stellar spectrum with a S/N of 200, but half of the photons originate in a featureless continuum generated by a disk. The depth and strength of the stellar lines would be reduced by about one half. This would be roughly equivalent to obtaining the spectrum of an undiluted star, but with half the S/N. If it is believed that continuum contamination is roughly equal to the stellar flux, then improving S/N might allow the detection of the stellar lines. Spectroscopic systems designed to be used with adaptive optics would reduce the contamination from extended emission and increase the likelihood of detecting stellar features. In cases where there may be significant thermal contamination, classification should not be based on equivalent width measures alone, but by the relative behavior of critical line pairs (see §5.2).

Ignoring for a moment contamination from nebular or circumstellar emission, what advice might we

give to those interested in doing a more accurate spectral analysis in the NIR? Unfortunately, the resolution and S/N limits required are a function of the stars spectral type, luminosity class and rotational velocity (something the researcher does not know at the start!) and whether one wishes to use a simple classification scheme or a full blown profile analysis. This is realized when one looks closely at the line strengths among the O dwarfs. In Figure 13, we plot the central region of the H -band, which happens to contain a Hydrogen line as well as neutral and ionized Helium. To create this figure, we created a set of low S/N line-free spectral regions from our data. These have been multiplied against are true spectra to illustrate the effect of reduced S/N on the detection of these weak stellar features. All the spectral features shown are $< 2 \text{ \AA}$ in strength, the strongest line being the HeI line at $1.70 \mu\text{m}$ in the O9 V star HD 149757 (e.w. = 1.8 \AA). Once the S/N was reduced to 150, the weak (0.45 \AA) HeII feature at $1.693 \mu\text{m}$ in HD 217086, is no longer confidently detected. For nearly all early O stars, we suggest a $S/N > 150$ for a quantitative analysis, to detect the very weak features and properly match the wings in the line. For late-O and B stars, such as in HD 149757, keeping $S/N > 100$ should be sufficient for their slightly stronger lines. Crude classification can still be obtained with a S/N under 100, but just barely. Only the strongest lines, $EW > 2.0 \text{ \AA}$ can be confidently detected once the S/N drops to 50 (Fig. 13).

For a proper profile analysis (and to resolve blends important in diagnosing luminosity classes) a resolution of at least $\lambda/\delta\lambda > 5000$ should be adhered to. Such a resolution is well matched for many if not most OB stars, which typically possess fairly high rotational rates ($V\sin i > 100 \text{ km/s}$). However, for OB stars with low rotation ($V\sin i < 100 \text{ km/s}$), a resolution of perhaps 8,000 or more will be needed to resolve their underlying profile (see, for instance, the slow rotator, HD 149438, Tau Sco, in Fig. 3). While seemingly high (by NIR standards!), these resolutions are really very low. Similar studies on cooler stars require much higher resolutions of several to many tens of thousands for a proper analysis (e.g., Luck & Heiter 2005).

5.2. The use of equivalent width for classification

In nearly all previous NIR spectral atlases, enormous tables and figures are given showing the equivalent width of strategic lines as a function of spectral type or luminosity class. Such measures have been critical to the development of a classification tool for the NIR. However, we do not present such tables here. The spectra in this atlas differ greatly from previous atlases, and thus dictates a different mind set for their use. We suggest that when working with high S/N and moderate to high resolution spectra, even without the use of quantitative profile analysis, one must adopt the philosophy outlined decades ago for the classification of stars in the optical. Here classification is based on *the comparison of spectra*; that between stars of known spectral and luminosity class and stars which are unknown. Important for a proper comparison, the resolution and approximate S/N of the stars being compared must be the same. What has been sorrowfully missing, however, in most NIR spectral classification programs has been **spectroscopic standards**. There isn't a single, conscientious optical spectroscopist doing classification work that would dream of skipping the step of taking classification standards. This is for a field for which optical classification spectra must number in the millions. In the infrared, researchers are relying on the scant, 100 or so O stars observed to date, to make crude comparisons to their own, independently obtained NIR spectra. This level of crude judgment to derive temperature and luminosity should not be tolerated if NIR classification is to become a robust technique. Moreover, as mentioned in §5.1, thermal contamination, something most optical astronomers do not typically deal with, makes classification via equivalent width strengths a very risky method for some applications.

The importance of obtaining ones own set of classification standards was recently highlighted in a study

by Bik et al. (2005b). They obtained high S/N, moderate resolution NIR spectra of ionizing stars of IRAS selected young star forming regions. Within the realm of this study, the researchers obtained spectra for a number of known O and early-B dwarf stars, using the identical spectroscopic set up and typical S/N obtained for their heavily reddened ionizing sources. They found a small but significant difference in the line strengths of their standard stars compared to previous lower resolution, lower S/N NIR atlases. Without the ability to calibrate with their own set of classification standards, they would have miss-classified most of their sources.

Looking again to the optical for guidance, most classifications criteria are based on the comparison of two lines in a spectrum. Typically, sub-classes are defined by when a set of lines are of equal strength, one line is stronger than the other, or when a line first appears or disappears, etc. (Jaschek & Jaschek 1987). While at first this method may appear crude, it in fact makes for a highly repeatable (from person to person) evaluation and is the crux to the success of the optical classification system. In the NIR we do not have such a wealth of diagnostic lines to allow for comparisons between oppositely behaving spectral features over all temperature and luminosity ranges of interest. The He lines do offer such a system to constrain temperature once O stars get cool enough to show HeI, and before they get too cool to show HeII (over the very narrow range of O7 to about O9.5). However, when including comparisons with other lines, CIV, Br γ , reasonable estimations appear possible. We have tried to outline just those comparisons within this paper (§4.2), though we admit, the field of NIR spectral classification is still very young. Still more observations are need to establish “typical” spectroscopic behavior in the NIR.

6. CONCLUSIONS

We present intermediate resolution ($R \sim 8,000 - 12,000$) high S/N H - and K -band spectroscopy of a sample of optically visible O and early-B stars. The purpose of this study is to better characterize OB spectral profiles in the NIR. We have also established some observational limits for researchers preparing to use a quantitative analysis to derive stellar temperature and luminosity with NIR spectra alone. In order to directly determine effective temperatures and $\log g$ for individual stars, one needs to work with atmospheric model codes which rely on profile fits. Such programs have recently been developed and show great promise (Lenorzer et al. 2004; Repolust et al. 2005). For most stars, a S/N > 100 and resolution of $r \approx 5000$ should be just sufficient. However, if the targets of interest turn out to be early-O, or have a very low rotational velocity, a higher S/N (> 150) or resolution ($R > 8000$), respectively, will need to be obtained.

When NIR spectral classification is sought, we *strongly encourage researchers to obtain spectra of known OB stars* for direct comparisons to their target stars. Until a time when equivalent “MK” standards are developed in the NIR, optically studied and thus known to be ‘well-behaved’ stars which bracket the expected spectral and luminosity range of the targets should be sufficient for this purpose.

We gratefully acknowledge the Subaru and VLT Observatories for their support of our program. This research has made use of the NASA’s Astrophysics Data System Bibliographic Services and the SIMBAD database operated at CDS (Strasbourg, France). MMH and MAK gratefully acknowledge support for this program from the National Science Foundation under Grant AST-0094050 to the University of Cincinnati.

Facilities: VLT:Antu (ISAAC), Subaru (IRCS)

A. Appendix

While not part of the original science goals of this program, the extraordinary spectral resolution and signal-to-noise achieved on all stars in this study, including the standard stars, seemed too good to go unpublished. Both for illustrative purposes, as well as for use by those looking to model and remove Brackett series transitions from their A-dwarf telluric standard stars, we provide spectra for all the A dwarf stars observed as part of the Subaru-IRCS program. Table A.1 gives the stars and spectral types, Figure 14 shows the spectra. Because we intend for these spectra to be used as templates, we have removed most of the high order noise features artificially. This was not done in the OB spectra because we did not want to inadvertently alter their very weak profiles.

The stars in Figure 14 have been arranged first by spectral class (all are dwarfs), and next by rotational velocity. Over even this small sample, it's clear that in modeling (to remove) Brackett features in A-dwarf stars, knowing the rotational velocity is at least as important as knowing the spectral type. The profile differences are small compared to the differences seen as a function of rotational velocity.

REFERENCES

- Bik, A., Lenorzer, A., Kaper, L., Comerón, F., Waters, L.B.F.M., de Koter, A., Hanson, M.M. 2003, A&A, 404, 249
- Bik, A., Kaper, L., Waters, L.B.F.M. 2005a, A&A, in press
- Bik, A., Kaper, L., Hanson, M.M., Smits, M., 2005b, A&A, in press
- Blum, R.D., Ramond, T.M., Conti, P.S., Figer, D.F. & Sellgren, K. 1997, AJ, 113, 1855
- Blum, R.D., Daminieli, A., Conti, P.S. 1999, AJ, 117, 1392
- Blum, R.D., Daminieli, A., Conti, P.S. 2001, AJ, 121, 3149
- Clark, J.S., Charles, P.A., Clarkson, W.I., Coe, M.J. 2003, A&A, 400, 655.
- Fickenscher, M.A., Hanson, M.M., Puls, J., 2004, AAS, 205, 2405
- Figer, D.F., Najarro, F., Geballe, T.R., Blum, R.D., Kudritzki, R.-P. 2005, ApJ Letters, accepted.
- Ghez, A.M., Duchêne, G., Matthews, K., et al. 2003, ApJ, 586, L127
- Hanson, M. M., Conti, P. S., Rieke, M. J. 1996, ApJS, 107, 281
- Hanson, M. M., Conti, P.S., Howarth, I.A. 1997, ApJ, 489, 698
- Hanson, M.M., Rieke, G.H. & Luhman, K.L. 1998, AJ, 116, 1915
- Ivanov, V. D., Rieke, M.J., Engelbracht, C.W., et al. 2004, ApJS, 151, 387.
- Jascheck, C. & Jaschek, M. 1987. *The Classification of Stars*. Cambridge: Cambridge Univ. Press
- Kenworthy, M.A. & Hanson, M.M. 2004, PASP, 116, 97
- Kudritzki, R. -P. & Puls, J. 2000, ARA&A, 38, 613

- Lenorzer, A., Vandenbussche, B., Morris, P. et al., 2002, *A&A*, 384, 473
- Lenorzer, A., Mokiem, M.R., de Koter, A., Puls, J. 2004, *A&A* 422, 275
- Luck, R.E., Heiter, U., 2005, *AJ*, 129, 1063
- Martì, J., Mirabel, I.F., Chaty, S., Rodriguez, L.F. 2000, *A&A*, 356, 943
- Massey, P., Lang, C., DeGioia-Eastwood, K., Garmany, C. 1995, *ApJ*, 438, 188
- Mirabel, I.F., Bandyopadhyay, R., Charles, P. A., et al. 1997, *ApJ*, 477, L45
- Moorwood, A.F. 1997, *Proc. SPIE*, 2871, 1146
- Morel, T. & Grosdidier, Y., 2005, *MNRAS*, 356, 665.
- Najarro, F., Hillier, D.J., Kudritzki, R.P. et al. 1994, *A&A* 285, 573
- Najarro, F., Krabbe, A., Genzel, R., Lutz, D., Kudritzki, R.P., Hillier, D.J. 1997, *A&A*, 325, 700.
- Najarro, F., in, 'Boulder-Munich II: Properties of Hot, Luminous Stars', ed. Ian Howarth, ASP Conference Series vol. 131 (San Francisco), 1998, p. 57
- Najarro, F., Figer, D.F., Hillier, D.J., Kudritzki, R.-P., *ApJ*, 611, L105
- Repolust, T., Puls, J., Hanson, M.M., Kudritzki, R.-P., Mokiem, M.R. 2005, *A&A*, submitted.
- Rousselot, P., Lidman, C., Cuby, J.-G., Moreels, G., Monnet, G. 2000, *A&A*, 354, 1134.
- Royer, F., Gerbaldi, M., Faraggiana, R., Gómez, A.E., 2002a, *A&A*, 381, 105.
- Royer, F., Grenier, S., Baylac, M.-O., Gómez, A.E., Zorec, J. 2002b, *A&A*, 393, 897
- Puls, J., Urbaneja, M., Springmann, U., et al. 2005, *A&A*, in press
- Tokunaga, A.T., Kobayashi, N., Bell, J., et al. 1998, *Proc. SPIE*, 3354, 512
- Walborn, N.R. & Fitzpatrick, E.L. 1990, *PASP*, 102, 379
- Wallace, L., & Hinkle, K. 1996, *ApJS*, 107, 312

Table 1. Sample and Observing Data

Star	SpType	2MASS H, K	$\alpha(2000)$	$\delta(2000)$	VLT-ISAAC ^a	Subaru-IRCS ^b
Cyg OB2 #7	O3 If*	6.8, 6.6	20 33 14.1	+41 20 22	...	Nov 01
Cyg OB2 #8A	O5.5 I(f)	5.7, 5.5	20 33 15.1	+41 18 50	...	July 02
Cyg OB2 #8C	O5 If	6.8, 6.5	20 33 18.1	+41 18 31	...	July 02
HD 5689	O6 V	8.3, 8.4	00 59 47.6	+63 36 28	...	Nov 01/July 02
HD 13268	ON8 V	7.9, 7.9	02 11 29.7	+56 09 32	...	Nov 01
HD 13854	B1 Iab	5.7, 5.6	02 16 51.7	+57 03 19	...	Nov 01
HD 13866	B2 Ib	7.1, 7.1	02 16 57.6	+56 43 08	...	July 02
HD 14134	B3 Ia	5.4, 5.3	02 19 04.5	+57 08 08	...	July 02
HD 14947	O5 If+	6.9, 6.9	02 26 47.0	+58 52 33	...	Nov 01
HD 15570	O4 If+	6.3, 6.2	02 32 49.4	+61 22 42	...	Nov 01
HD 15558	O5 III(f)	6.6, 6.5	02 32 42.5	+61 27 22	...	July 02
HD 15629	O5 V((f))	7.3, 7.3	02 33 20.6	+61 31 18	...	July 02
HD 30614	O9 Ia	4.4, 4.2	04 54 03.0	+66 20 34	...	Nov 01
HD 36166	B2 V	6.3, 6.3	05 29 54.8	+01 47 21	...	Nov 01
HD 37128	B0 Ia	2.4, 2.3	05 36 12.8	−01 12 07	...	Nov 01
HD 37468	O9.5 V	4.6, 4.5	05 38 44.8	−02 36 00	...	Nov 01
HD 46150	O5 V((f))	6.5, 6.4	06 31 55.5	+04 56 34	...	Nov 01
HD 46223	O4 V((f))	6.7, 6.7	06 32 09.3	+04 49 24	...	Nov 01
HD 64568	O3 V((f))	9.1, 9.1	07 53 38.2	−26 14 03	...	Nov 01
HD 66811	O4 I(n)f	3.0, 3.0	08 03 35.0	−40 00 11	...	Nov 01
HD 90087	O9.5 II	7.7, 7.8	10 22 20.9	−59 45 20	May 01	...
HD 92554	O9 II _n	9.1, 9.1	10 39 45.7	−60 54 40	May 01	...
HD 115842	B0.5 Ia	5.3, 5.2	13 20 48.3	−55 48 03	Apr 01	...
HD 123008	ON9.5 Iab	7.8, 7.7	14 07 30.6	−64 28 09	Apr 01	...
HD 134959	B2 Ia	5.5, 5.2	15 15 24.1	−59 04 29	Apr 01	...
HD 148688	B1 Ia	4.1, 4.1	16 31 41.8	−41 49 02	May 01	...
HD 149438	B0.2 V	3.5, 3.7	16 35 53.0	−28 12 58	...	July 02
HD 149757	O9.5 V	2.7, 2.7	16 37 09.5	−10 34 02	...	July 02
HD 154368	O9.5 Iab	4.9, 4.8	17 06 28.4	−35 27 04	Apr 01	...
HD 163181	BN0.5 Ia	5.1, 4.9	17 56 16.1	−32 28 30	Apr 01	...
HD 190864	O6.5 III	7.3, 7.3	20 05 39.8	+35 36 28	...	July 02
HD 191423	O9 III	7.7, 7.8	20 08 07.1	+42 36 22	...	July 02
HD 192639	O7 Ib	6.3, 6.2	20 14 30.4	+37 21 13	...	July 02
HD 203064	O7.5 III	5.1, 5.1	21 18 27.2	+43 56 45	...	July 02
HD 209975	O9.5 Ib	4.9, 4.9	22 05 08.8	+62 16 47	...	July 02
HD 210809	O9 Iab	7.4, 7.4	22 11 38.6	+52 25 48	...	July 02
HD 217086	O7 V	6.1, 6.0	22 56 47.2	+62 43 38	...	Nov 01

^aThe VLT-ISAAC H -band resolution is $R \sim 10,000$; the K -band resolution is $R \sim 8000$. The typical S/N ratios obtained with these spectra were $S/N \sim 100-150$, with areas as high as $S/N \sim 200$, and as low as $S/N \sim 50$, depending on the local telluric contamination

^bThe Subaru-IRCS H - and K -band band resolution is $R \sim 12,000$. The typical S/N ratios obtained with these spectra were $S/N \sim 200-300$, with areas as high as $S/N \sim 500$, and as low as $S/N \sim 100$, depending on the local telluric contamination

Table 2. The OB Star Sample

	V	III	II/Ib	Iab/Ia
O3	HD 64568			Cyg OB2 #7
O4	HD 46223			HD 66811, HD 15570
O5	HD 46150, HD 15629	HD 15558 (<i>K</i> -band only)		HD 14947, Cyg OB2 #8C Cyg OB2 #8A
O6	HD 5689	HD 190864		
O7	HD 217086	HD 203064	HD 192639	
O8	HD 13268			
O9	HD 37468, HD 149757	HD 191423	HD 92554 HD 90087, HD 209975	HD 30614, HD 210809 HD 123008, HD 154368 HD 37128
B0	HD 149438 (<i>K</i> -band only)			HD 115842, HD 163181
B1				HD 13854, HD 148688
B2	HD 36166		HD 13866	HD 134959
B3				HD 14134

Table A.1. Telluric Stars

Star	SpType	Vsin <i>i</i> (km/s) ^a
HD 12279	A1 Vn	275
HD 28780	A1 V	28
HD 146624	A0 V	39
HD 171149	A0 V	301
HD 199629	A1 V	217
HD 205314	A0 V	191

^aFrom Royer et al. (2002a, 2002b).

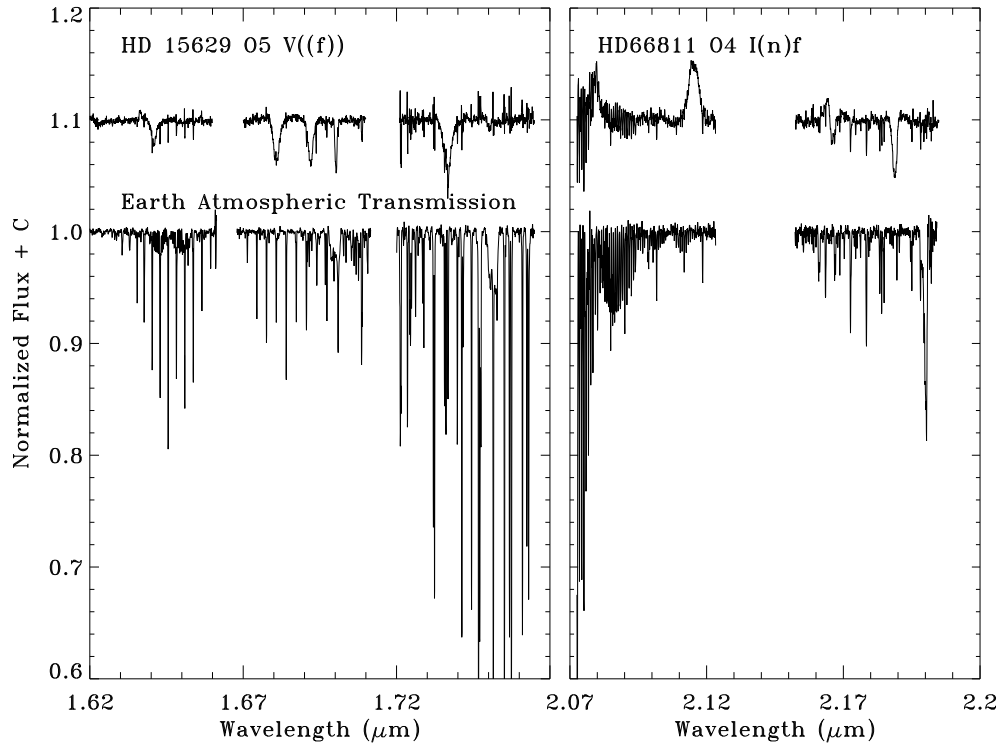


Fig. 1.— **Earth Telluric Lines.** The lower graph shows the wavelength dependence of the Earth’s transmission, normalized to 1 to show only the absorption in small structure lines. On top is shown the final reduced spectrum from two stars, HD15629 in the H -band and HD 66811 in the K -band. Telluric corrections can prove very challenging when there are either intermittent clouds (as was the case for HD 15629), or when the airmass is very large and suitable standards sampling such airmass are not available (as was the case for HD 66811). The numerous noise spikes seen in the stellar spectra can easily be traced back to very strong narrow telluric features in the Earth’s atmosphere.

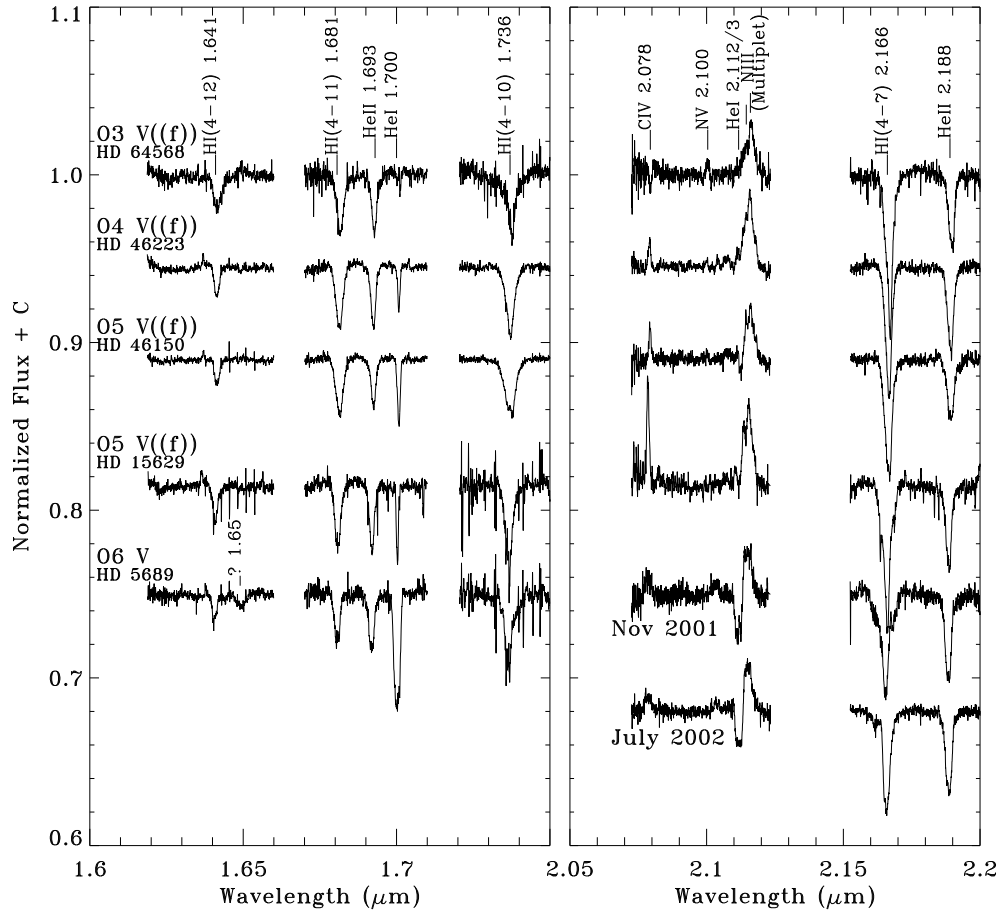


Fig. 2.— **Early-O Dwarf Stars.** Characteristic lines include strong HeII ($\lambda 1.693\mu\text{m}$, $2.188\mu\text{m}$), and among the hottest O3, no HeI nor CIV emission (though possibly CIV absorption). All early-O dwarf stars show NIII emission at $2.115\mu\text{m}$.

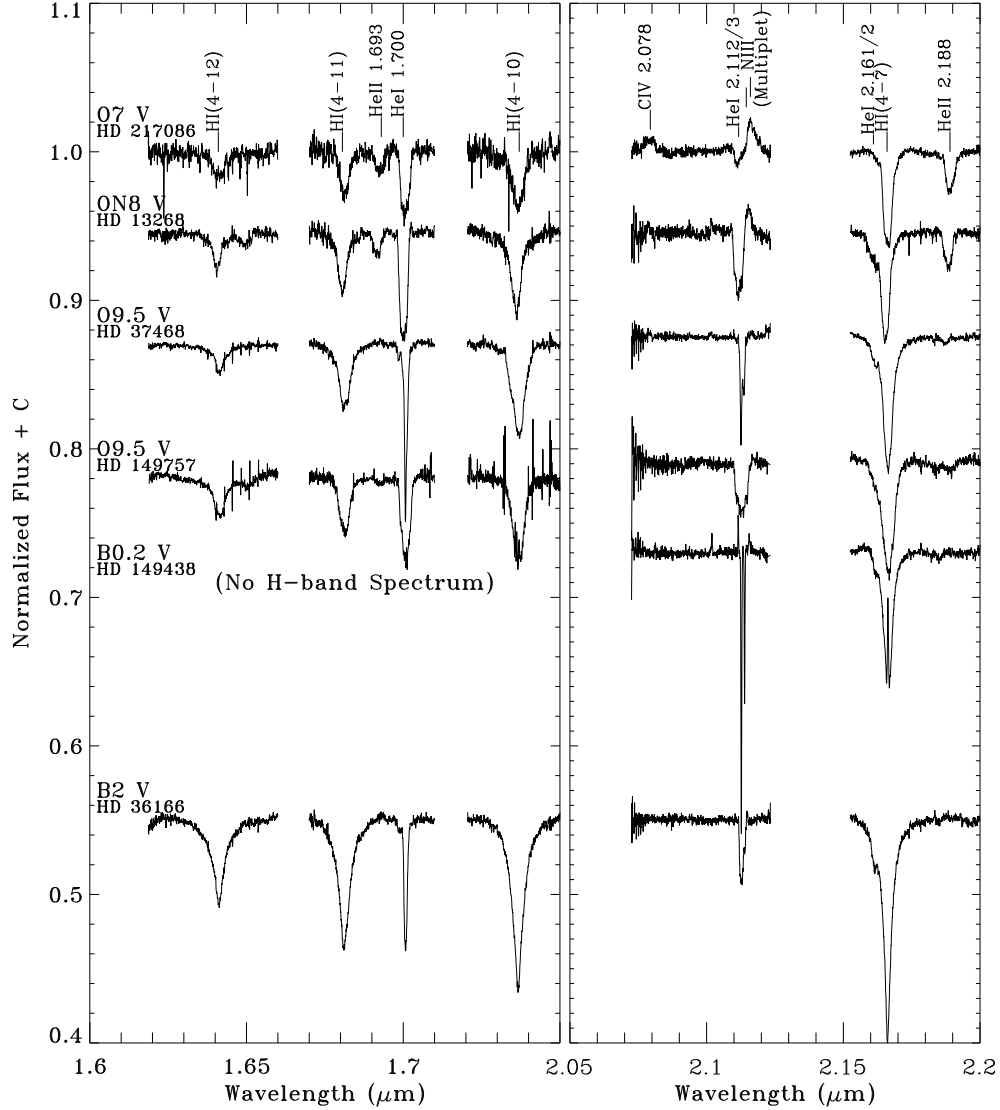


Fig. 3.— **Late-O Dwarf Stars.** Characteristic lines in late-O dwarfs include simultaneously occurring HeI and HeII. HeII disappears for B dwarfs (just as in the optical 4686\AA). We also see a rather strong HeI absorption developing in cooler B dwarfs. Note the very deep and narrow HeI absorption in HD 149438, a very slowly rotating star ($V\sin i \approx 10\text{-}20$ km/s).

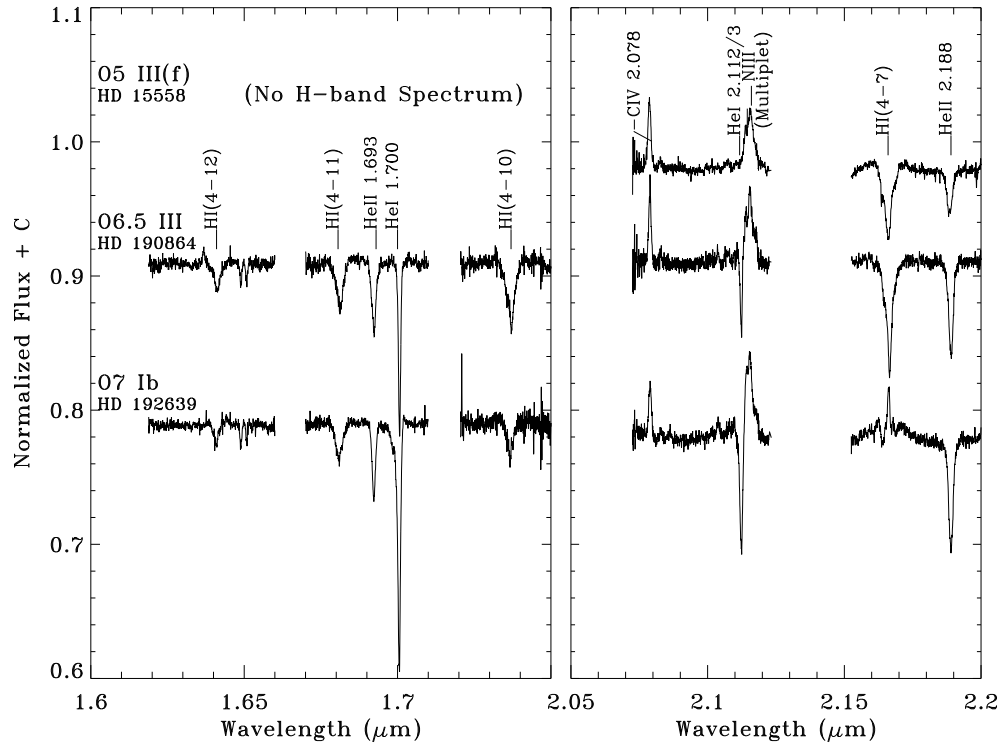


Fig. 4.— **Mid-O Giant Stars.** The effect of increased luminosity for this spectral range is most directly seen in deeper Brackett and HeI absorption, though the line width is further narrowed by the slow rotation rate of these stars.

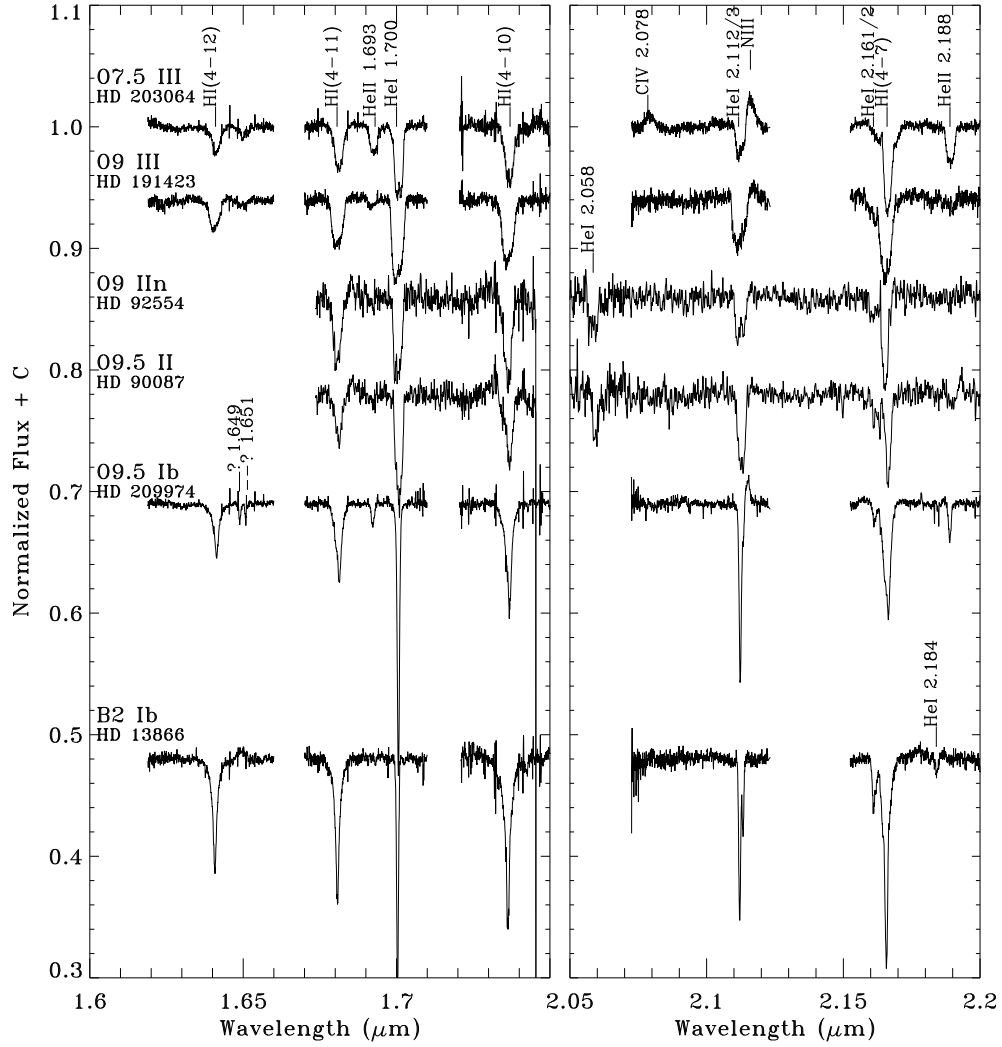


Fig. 5.— **Late-O and Early-B Giant Stars.** As shown in Fig. 3, these stars show a deepening of their Brackett and HeI lines, as compared to dwarf stars of the same spectral type. HeI, at $\lambda 2.184\mu\text{m}$ becomes apparent in early-B giants.

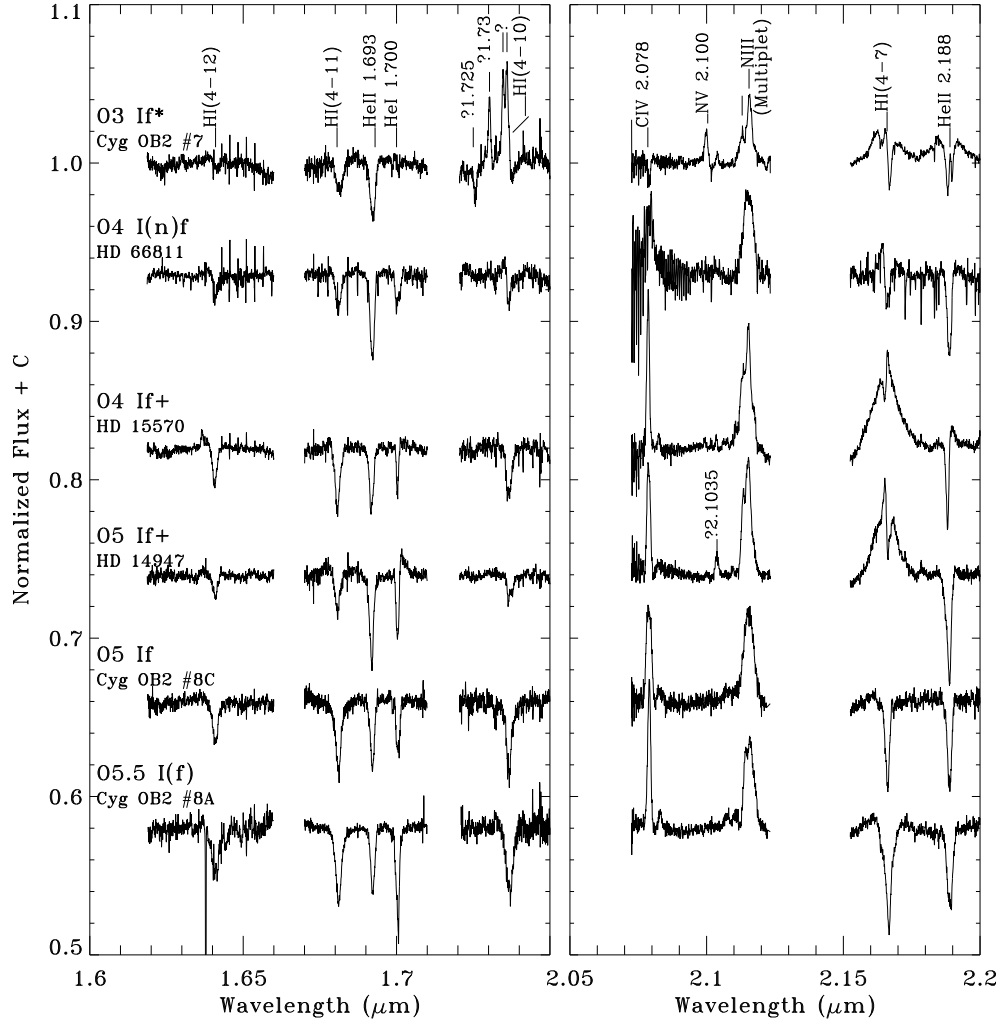


Fig. 6.— **Early-O Supergiant Stars.** In the most extreme early-O supergiants, Br γ becomes partly or wholly filled in, or in strong broad emission. Other signs of high luminosity for this spectral class include, the narrowing and deepening of the Brackett and Helium lines. The unidentified doublet features marked as “?” in Cyg OB2 #7 were found to lie at λ 1.7347,1.7360.

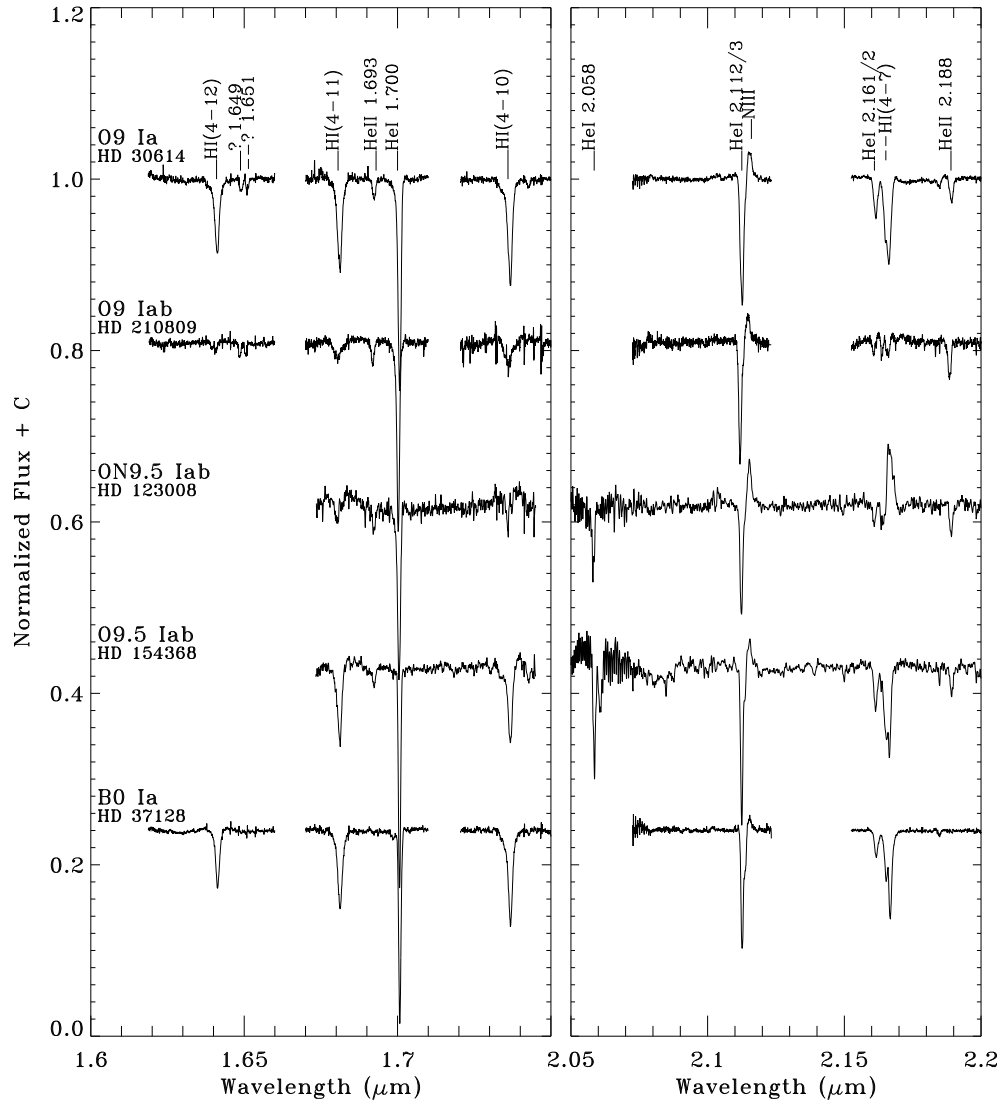


Fig. 7.— **Late-O Supergiant Stars.** Entirely unique to this range of temperature and spectral class is the appearance of weak, narrow HeI absorption at 2.161/2 μm . Both the HeI and Hydrogen Brackett lines have become extremely narrow and deep.

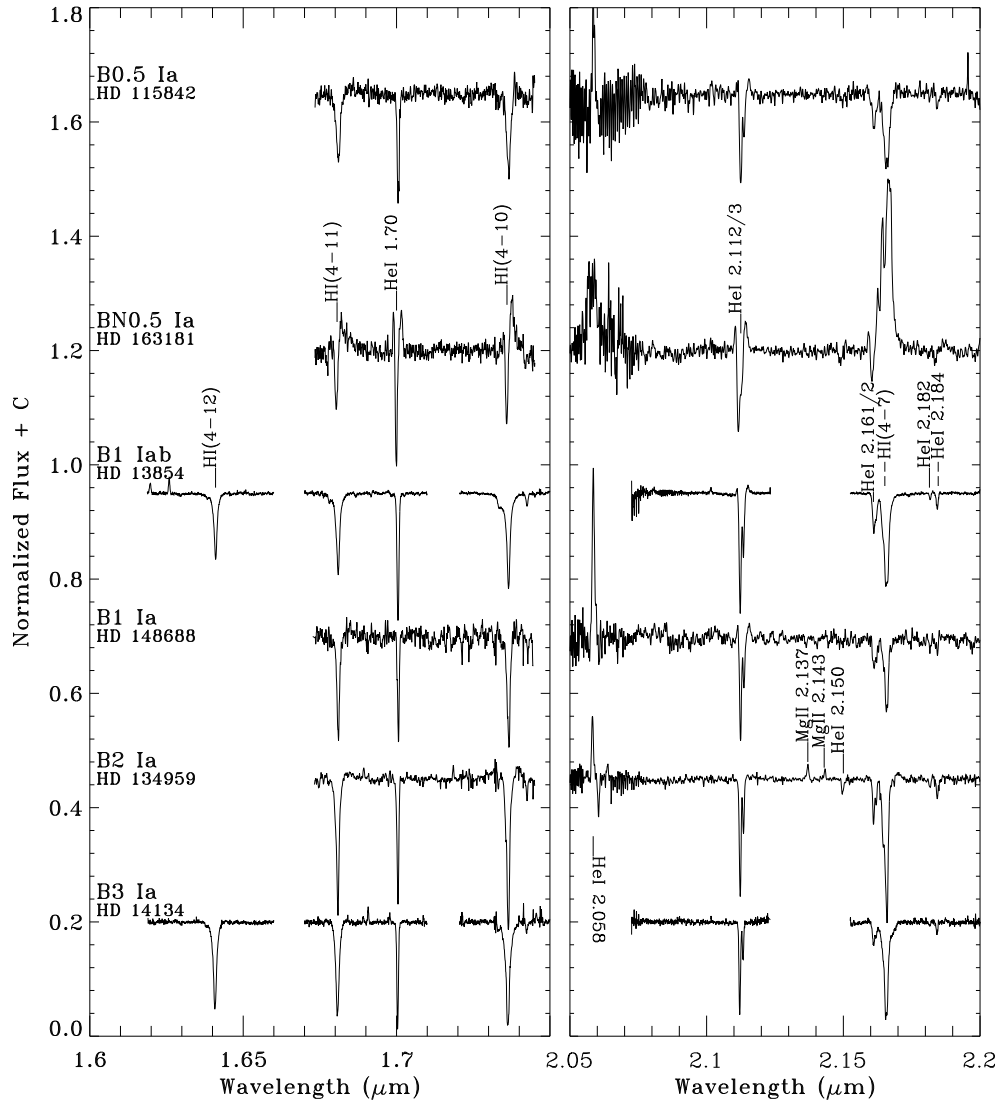


Fig. 8.— **Early-B Supergiant Stars.** As in Fig. 6, the HeI and Brackett lines become deep and narrow. However, distinct from their slightly hotter cousins, the early-B supergiants also show weak, but significant HeI absorption at $2.184\mu\text{m}$.

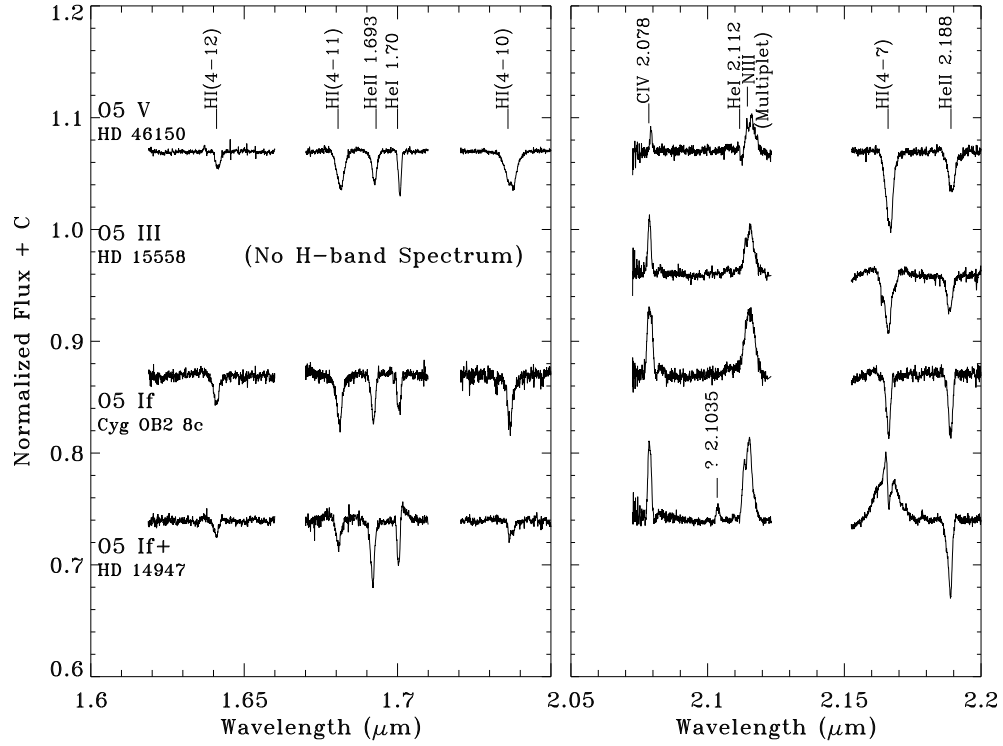


Fig. 9.— **Luminosity variations seen in O5 stars.** Deepening and narrowing of the Brackett line and loss of broad wings correlates with increased luminosity in O5 stars. In the most extreme O supergiants, $\text{Br}\gamma$ is in emission. Note the contamination of $\text{Br}12/11/10$ in HD14947 by wind-effects (see text §4.2).

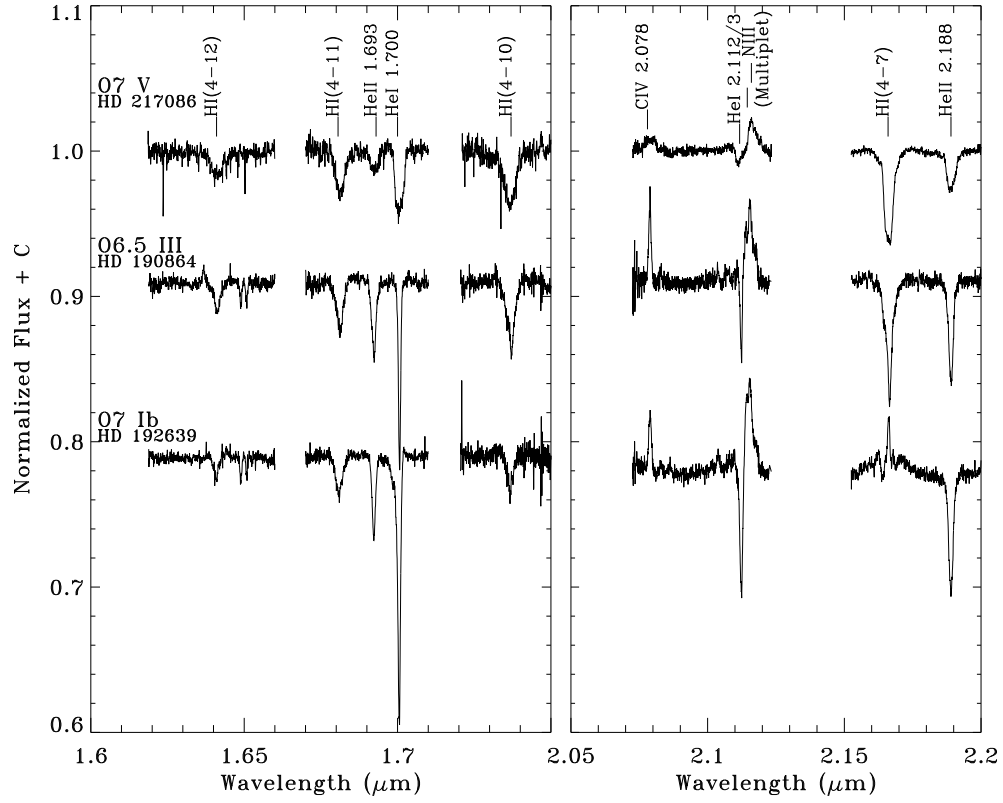


Fig. 10.— **Luminosity variations seen in O7 stars.** The same effects are seen in the O7 stars as was displayed in the O5 stars, in Fig. 9.

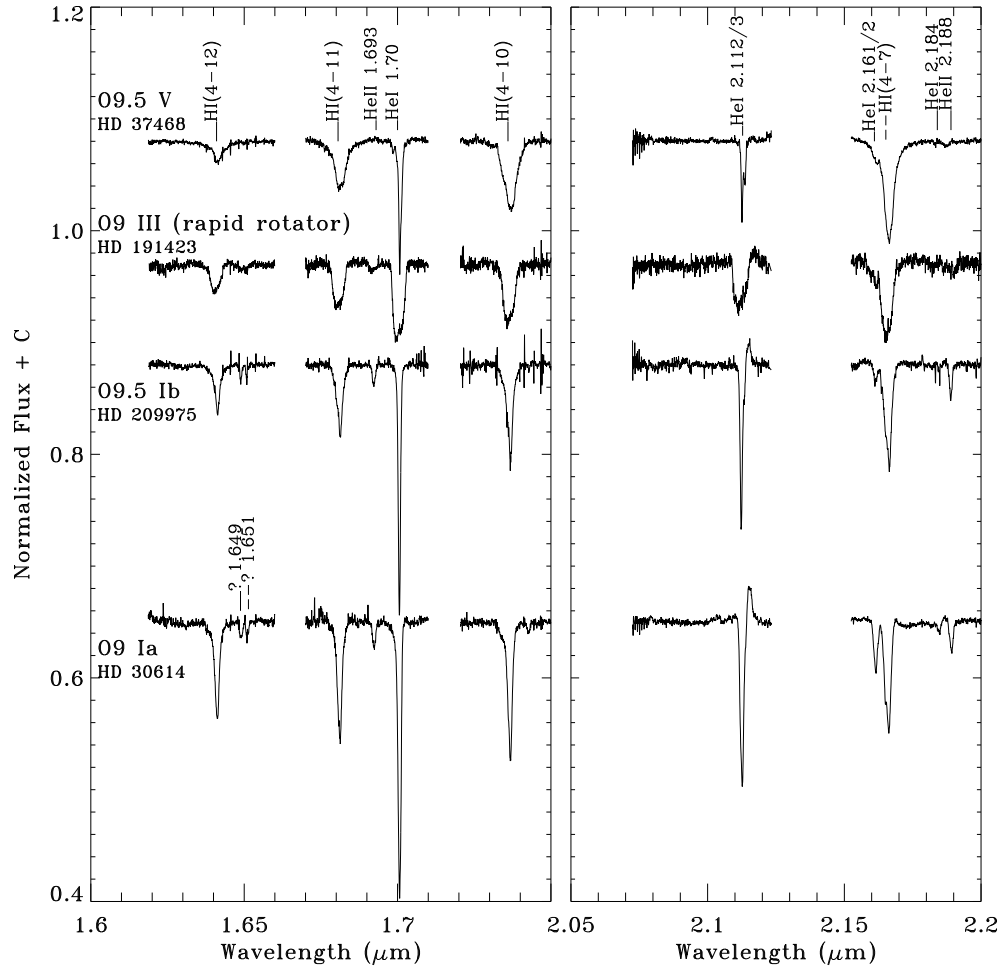


Fig. 11.— **Luminosity variations seen in O9 stars.** It is interesting to note that the O9 giant might be incorrectly classified as a dwarf, if it wasn't known to be a rapid rotator. The broad HeI at $1.700\mu\text{m}$ gives away its large $V\sin i$.

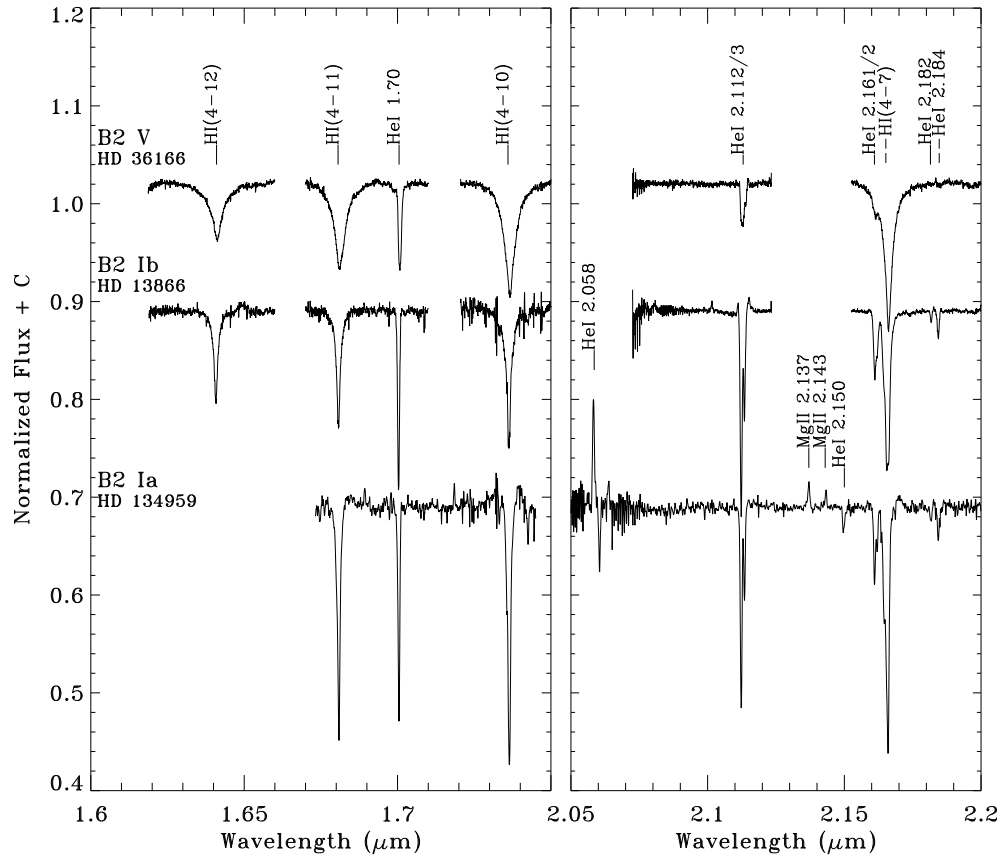


Fig. 12.— **Luminosity variations seen in B2 stars.** Lack of wings, deepening cores, presence of HeI at 2.161/2, 2.184μm all correlate with increased luminosity among early-B stars.

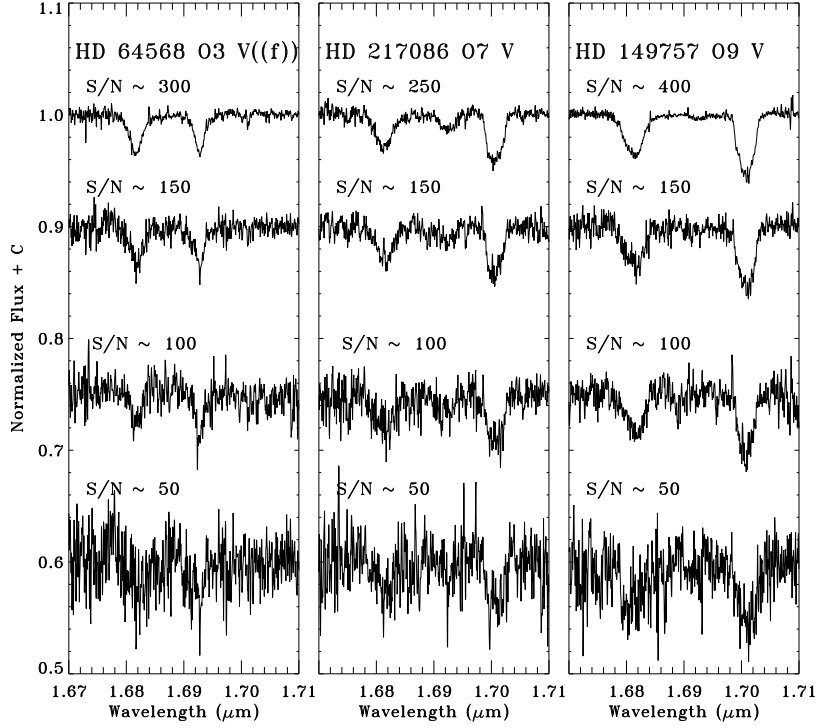


Fig. 13.— **The need for high signal-to-noise in OB star spectra.** This figure shows our final spectra plotted on the top of each panel. Below those spectra, the same spectra are given, but the S/N has been artificially reduced for illustrative purposes. Very high signal-to-noise, $S/N > 150$, will typically be required for a reliable quantitative analysis performed on the stellar profiles. The strength of features presented range from $e.w. = 0.42 \text{ \AA}$ for the $1.693 \text{ }\mu\text{m}$ HeII line in HD217068 to $e.w. = 1.8 \text{ \AA}$ for the $1.700 \text{ }\mu\text{m}$ HeI line in HD 149757. If the signal-to-noise drops much below 100, even spectral classification becomes unreliable, as features with strengths below $\sim 1.0 \text{ \AA}$ become undetectable.

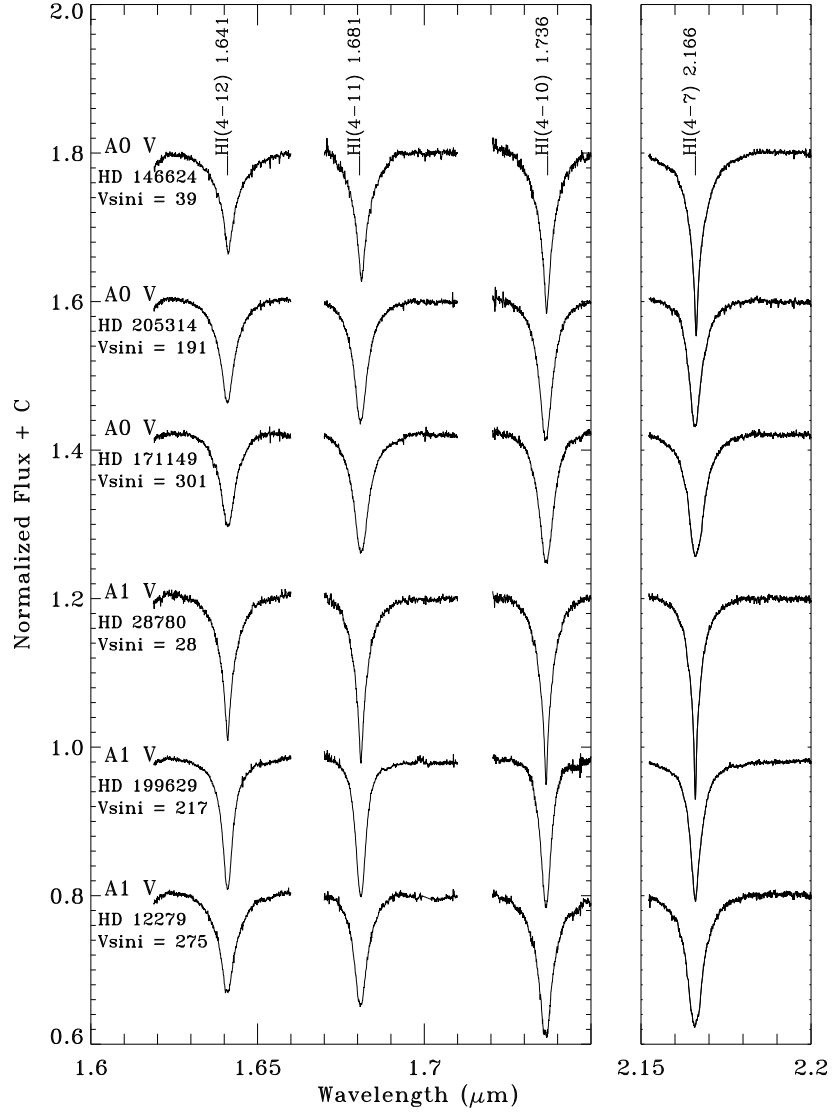


Fig. 14.— **A Dwarf stars useful for telluric standards.** Note the significant variation in profile characteristics with rotational velocity (velocities are expressed in km/s). High-order noise spikes, resulting from the telluric corrections, have been artificially removed.